

# Top-quark FCNC Productions at LHC in Topcolor-assisted Technicolor Model

Junjie Cao<sup>1,2</sup>, Guoli Liu<sup>3</sup>, Jin Min Yang<sup>4</sup>, Huanjun Zhang<sup>1,4</sup>

<sup>1</sup> *Department of Physics, Henan Normal University, Xinxiang 453007, China*

<sup>2</sup> *Physics Department, Technion, 32000 Haifa, Israel*

<sup>3</sup> *Service de Physique Theorique CP225, Universite Libre de Bruxelles, 1050 Brussels, Belgium*

<sup>4</sup> *Institute of Theoretical Physics, Academia Sinica, Beijing 100080, China*

We evaluate the top-quark FCNC productions induced by the topcolor assisted technicolor (TC2) model at the LHC. These productions proceed respectively through the parton-level processes  $gg \rightarrow t\bar{c}$ ,  $cg \rightarrow t$ ,  $cg \rightarrow tg$ ,  $cg \rightarrow tZ$  and  $cg \rightarrow t\gamma$ . We show the dependence of the production rates on the relevant TC2 parameters and compare the results with the predictions in the minimal supersymmetric model. We find that for each channel the TC2 model predicts a much larger production rate than the supersymmetric model. All these rare productions in the TC2 model can be enhanced above the  $3\sigma$  sensitivity of the LHC. Since in the minimal supersymmetric model only  $cg \rightarrow t$  is slightly larger than the corresponding LHC sensitivity, the observation of these processes will favor the TC2 model over the supersymmetric model. In case of unobservation, the LHC can set meaningful constraints on the TC2 parameters.

PACS numbers: 14.65.Ha, 12.60.Fr, 12.60.Jv

**Introduction:** It is well known that flavor-changing neutral-current (FCNC) processes have been a crucial test of the Standard Model (SM) and a good probe for new physics beyond the SM. As the heaviest fermion in the SM, the top quark may play a special role in such FCNC phenomenology. In the SM the top quark FCNC interactions are extremely suppressed [1] and impossible to be detected in current and foreseeable colliders. In contrast to the SM, the new physics models often predict much larger FCNC top quark interactions [2]. Such large FCNC top quark interactions are so far allowed by current experiments since the Tevatron collider only gave some rather loose bounds on the FCNC top quark decays due to the small statistics [3]. The future colliders like the LHC will allow a precision test for the top quark properties including the FCNC interactions [4].

Once the measurement of the FCNC top quark processes is performed at the LHC, some new physics models can be immediately tested. For example, the FCNC top quark decays and top-charm associated productions were found to be significantly enhanced in the minimal supersymmetric model [5, 6] and technicolor models [7, 8].

Although so far in the literature there are many papers devoting to the new physics predictions for the FCNC top quark productions at the LHC, usually different processes are treated in different papers. Since these FCNC processes are correlated in a given new physics model, it is necessary to give a comprehensive study of all these processes in one paper. Recently, such an effort was given for the popular supersymmetric models [9]. In this work we perform a comprehensive analysis for the FCNC top quark productions in TC2 model. We will consider the

production channels

$$gg \rightarrow t\bar{c}, cg \rightarrow t, cg \rightarrow tg, cg \rightarrow tZ, cg \rightarrow t\gamma \quad (1)$$

Some of these processes have been studied in the literature:  $gg \rightarrow t\bar{c}$  was studied in the second and third papers in [7], but only the  $s$ -channel contributions were considered;  $cg \rightarrow tV$  ( $V$  is a vector boson) were studied in [10], but all box diagrams were ignored. The other process  $cg \rightarrow t$  in TC2 model has not been studied in the literature. In this work we consider all these productions and compare their rates. Also, we will compare the TC2 results with the predictions of supersymmetric models. Note that in our studies the parton-level processes will be used to label the corresponding hadronic productions and the charge-conjugate channel for each production is also included.

**About TC2 Model:** Before our calculations we recapitulate the basics of TC2 model. As is well known, the fancy idea of technicolor tries to provide an elegant dynamical mechanism for electroweak symmetry breaking, but it encounters great difficulty when trying to generate fermion masses, especially the heavy top quark mass. The TC2 model [11] combines technicolor interaction with topcolor interaction, with the former being responsible for electroweak symmetry breaking and the latter for generating large top quark mass. This model so far survives current experimental constraints and remains one of the candidates of new physics.

The TC2 model predicts a number of pseudo-Goldstone bosons like the top-pions ( $\pi_t^0$  and  $\pi_t^\pm$ ) at the weak scale [11]. The top quark interactions are altered with respect to the SM predictions since it is treated

differently from other fermions in TC2 model. For example, the TC2 model predicts some anomalous couplings for the top quark, such as the tree-level FCNC coupling  $t\bar{c}\pi_t^0$  and the charged-current  $t\bar{b}\pi_t^-$  coupling given by

$$\begin{aligned} & \frac{(1-\epsilon)m_t}{\sqrt{2}F_t} \frac{\sqrt{v^2 - F_t^2}}{v} (iK_{UL}^{tt}K_{UR}^{tt}\bar{t}L t R \pi_t^0 \\ & + \sqrt{2}K_{UR}^{tt}K_{DL}^{bb}\bar{t}R b_L \pi_t^- + iK_{UL}^{tt}K_{UR}^{tc}\bar{t}L c_R \pi_t^0 \\ & + \sqrt{2}K_{UR}^{tc}K_{DL}^{bb}\bar{c}R b_L \pi_t^- + K_{UL}^{tt}K_{UR}^{tt}\bar{t}L t R h_t^0 \\ & + K_{UL}^{tt}K_{UR}^{tc}\bar{t}L c_R h_t^0 + h.c.), \end{aligned} \quad (2)$$

where the factor  $\sqrt{v^2 - F_t^2}/v$  ( $v \simeq 174$  GeV) reflects the effect of the mixing between the top-pions and the would-be Goldstone bosons [12].  $K_{UL}$ ,  $K_{DL}$  and  $K_{UR}$  are the rotation matrices that transform respectively the weak eigenstates of left-handed up-type, down-type and right-handed up-type quarks to their mass eigenstates, whose values can be parameterized as [7]

$$K_{UL}^{tt} \simeq K_{DL}^{bb} \simeq 1, \quad K_{UR}^{tt} \simeq \frac{m'_t}{m_t} = 1 - \epsilon, \quad (3)$$

$$K_{UR}^{tc} \leq \sqrt{1 - (K_{UR}^{tt})^2} = \sqrt{2\epsilon - \epsilon^2}, \quad (4)$$

with  $m'_t$  denoting the topcolor contribution to the top quark mass. In Eq.(2) we neglected the mixing between up quark and top quark. Note that in TC2 model a CP-even scalar called top-Higgs ( $h_t^0$ ) may also exist, whose couplings are similar to the neutral top-pion[7].

The parameters involved in our calculations are: the masses of the top-pions and top-Higgs, the parameter  $K_{UR}^{tc}$ , the top-pion decay constant  $F_t$  and the parameter  $\epsilon$ , which parameterizes the portion of the extended-technicolor contribution to the top quark mass. In our study we take  $m_t = 180.7$  GeV [13] and  $F_t = 50$  GeV. Since the mass splitting between neutral and charged top-pion is very small, we assume  $m_\pi^0 = m_\pi^\pm$ . The top-pions mass is model-dependent and is usually of a few hundred GeV [11]. About the top-Higgs mass, ref. [7] gave a lower bound of about  $2m_t$ , but it is an approximate analysis and the mass below  $t\bar{t}$  threshold is also possible [14]. In our analysis we assume

$$m_{\pi_t^0} = m_{\pi_t^\pm} = m_{h_t^0} \equiv M_{TC}. \quad (5)$$

**Calculations:** For the parton-level processes in eq.(1) we only plot the Feynman diagrams in Figs. 1 and 2 for  $gg \rightarrow t\bar{c}$  and  $cg \rightarrow tZ$ , respectively. Other processes have similar Feynman diagrams which can be easily obtained from Figs. 1 and 2. For example,  $cg \rightarrow tg$  can be straightforwardly obtained from Fig. 1, and  $cg \rightarrow t\gamma$  can be obtained from Fig.2 by removing some diagrams with non-exist vertices. The calculations for these production processes are straightforward. Here we take the calculation of  $gg \rightarrow t\bar{c}$  as an example. Its amplitude takes the

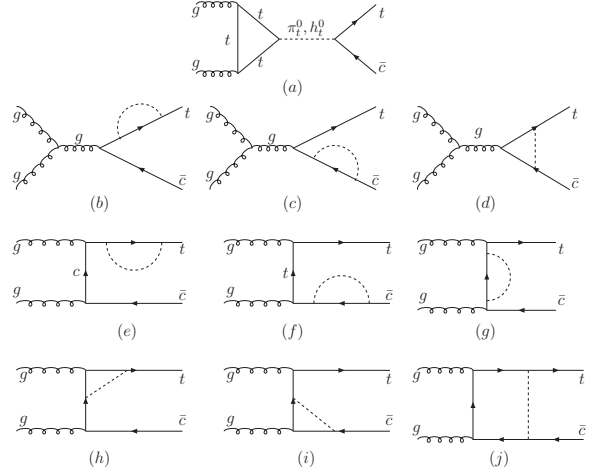


FIG. 1: Feynman diagrams for  $gg \rightarrow t\bar{c}$  in TC2 model. The boson in each loop denotes a neutral top-pion, top-Higgs or a charged top-pion, while the fermion in each loop can be a top or bottom quark depending on the involved boson being neutral or charged.

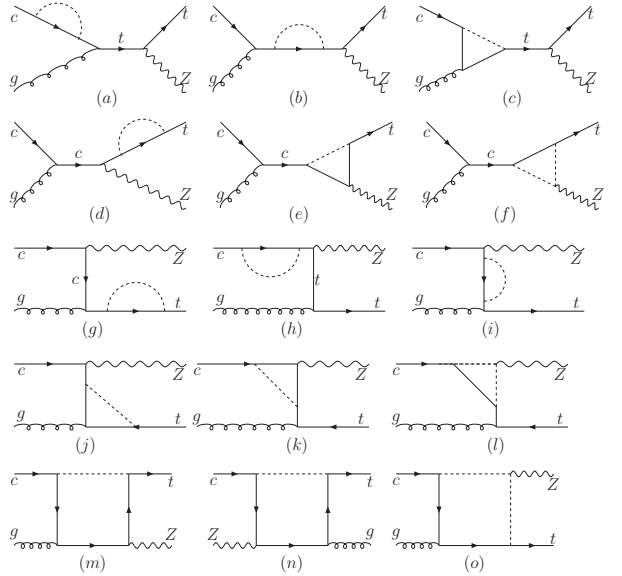


FIG. 2: Feynman diagrams for  $cg \rightarrow tZ$  in TC2 model. The boson in each loop denotes a neutral top-pion, top-Higgs or a charged top-pion, while the fermion in each loop can be a top or bottom quark depending on the involved boson being neutral or charged.

form

$$\begin{aligned} & \frac{g_s^2 m_t^2}{2F_t^2} \frac{v^2 - F_t^2}{v^2} K_{UR}^{tt} K_{UR}^{tc} \epsilon_\mu(k_1) \epsilon_\nu(k_2) \\ & \times \sum_i T^i \bar{u}(p_t) \Gamma_i^{\mu\nu} P_R v(p_c), \end{aligned} \quad (6)$$

where the sum is over all the Feynman diagrams in Fig. 1,  $T_i$  are color factors,  $P_R = (1 + \gamma_5)/2$ ,  $k_{1,2}$  denote the mo-

momentum of two incoming gluons and  $p_{t,c}$  the momentum of outgoing top and anti-charm quarks, and  $\Gamma_i^{\mu\nu}$  is given by

$$\begin{aligned} & c_1^i p_t^\mu p_c^\nu + c_2^i p_c^\mu p_c^\nu + c_3^i p_t^\mu p_c^\nu + c_4^i p_t^\nu p_c^\mu + c_5^i p_t^\mu \gamma^\nu + c_6^i p_c^\mu \gamma^\nu \\ & + c_7^i p_c^\nu \gamma^\mu + c_8^i p_t^\nu \gamma^\mu + c_9^i g^{\mu\nu} + c_{10}^i \gamma^\mu \gamma^\nu + c_{11}^i p_t^\mu p_t^\nu k_2 \\ & + c_{12}^i p_c^\mu p_c^\nu k_2 + c_{13}^i p_t^\mu p_c^\nu k_2 + c_{14}^i p_t^\nu p_c^\mu k_2 \\ & + c_{15}^i p_t^\mu \gamma^\nu k_2 + c_{16}^i p_c^\mu \gamma^\nu k_2 + c_{17}^i p_c^\nu \gamma^\mu k_2 \\ & + c_{18}^i p_t^\nu \gamma^\mu k_2 + c_{19}^i g^{\mu\nu} k_2 + c_{20}^i i \varepsilon^{\mu\nu\alpha\beta} \gamma_\alpha k_{2\beta}. \end{aligned} \quad (7)$$

Here the coefficients  $c_j^i$  are obtained by the straightforward calculation of each Feynman diagram in Fig. 1, which are composed of scalar loop functions [15] and can be calculated by using LoopTools [16]. The calculations of the loop diagrams are tedious and the analytical expressions for the coefficients  $c_j^i$  are lengthy, so we do not present the explicit expressions of  $c_i$ s here.

The hadronic cross section at the LHC is obtained by convoluting the parton cross section with the parton distribution functions. In our calculations we use CTEQ6L [17] to generate the parton distributions with the renormalization scale  $\mu_R$  and the factorization scale  $\mu_F$  chosen to be  $\mu_R = \mu_F = m_t$ . To make our predictions more realistic, we applied some kinematic cuts. For example, we require that the transverse momentum of each produced particle larger than 15 GeV and its pseudo rapidity less than 2.5 in the laboratory frame. For  $cg \rightarrow t$  followed by  $t \rightarrow Wb$ , we do not require the top quark exactly on mass shell and instead we require the invariant mass of bottom quark and  $W$ -boson in a region of  $m_t - 3\Gamma_t \leq M_{bW} \leq m_t + 3\Gamma_t$  ( $\Gamma_t$  is the top quark width). This requirement was used in [18] to investigate the observability of this channel at hadron colliders in the effective Lagrangian framework.

**Numerical results:** Since the cross section for each channel is simply proportional to  $K_{UR}^{tc}$  as shown in eq.(6), here we do not show the dependence on  $K_{UR}^{tc}$ . We will fix  $K_{UR}^{tc} = 0.4$  and show the dependence on  $M_{TC}$ . In Fig. 3 we show the hadronic cross section of the production proceeding by the parton-level process  $gg \rightarrow t\bar{c}$  versus  $M_{TC}$ , where the  $s$ -channel and non- $s$ -channel contributions are shown separately. From Fig. 3 we see that the contributions are dominated by the  $s$ -channel process for a heavy top-pion and there exist three regions of  $M_{TC}$ . In the range  $m_t < M_{TC} < 2m_t$ , the cross section is maximal and can reach about 30 pb. The reason is that in this region  $t\bar{c}$  is the dominant decay mode of  $\pi_t^0$  and  $h_t^0$  which can be produced on-shell through the  $s$ -channel. When  $M_{TC}$  passes the threshold of  $2m_t$  and keeps increasing, the cross section drops quickly since the  $t\bar{t}$  is becoming the dominant decay mode of  $\pi_t^0$  and  $h_t^0$ . In the light mass region  $M_{TC} < m_t$ , which is disfavored by  $R_b$  [19], the non- $s$ -channel contributions are dominant and the  $s$ -channel contributions are suppressed since the top-pion and the top-Higgs in the  $s$ -channel cannot be produced on-shell.

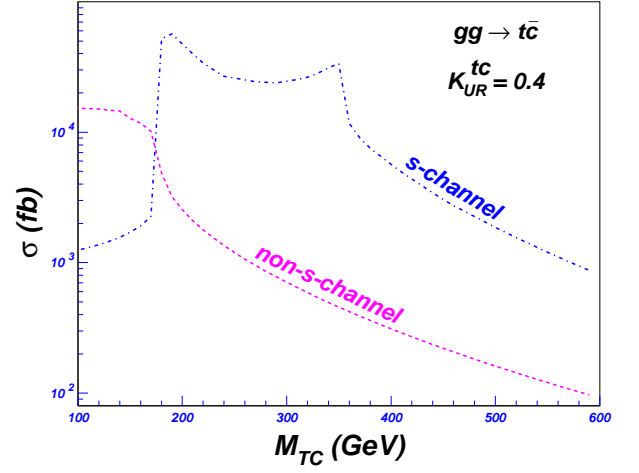


FIG. 3: The hadronic cross section of the production proceeding through  $gg \rightarrow t\bar{c}$  versus  $M_{TC}$ .

The total hadronic cross sections for all these processes are plotted in Fig.4 for comparison. We see that the production proceeding through  $gg \rightarrow t\bar{c}$  has the largest rate for a heavy top-pion. Of course, the productions in the two channels of  $gg \rightarrow t\bar{c}$  and  $cg \rightarrow tg$  cannot be distinguished from each other since the charm quark jet cannot be distinguished from the gluon jet. Therefore, the cross sections of these two channels should be summed, which gives a signal of an energetic lepton (electron or muon) plus two jets (one of them is  $b$ -jet) plus missing energy.

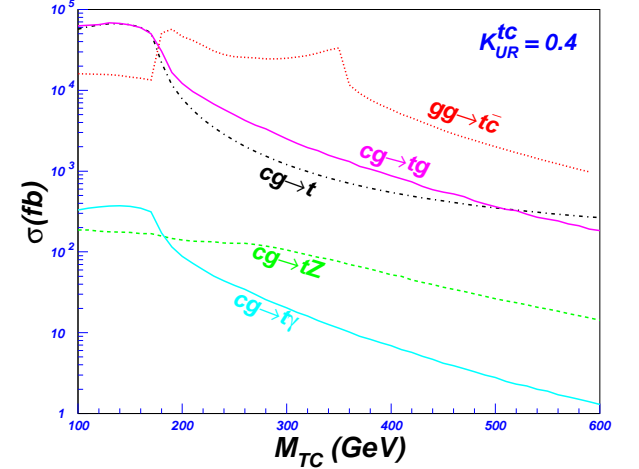


FIG. 4: The hadronic cross sections of the productions proceeding through the parton-level processes labelled on each curve.

Now we compare the TC2 predictions with the predictions in supersymmetric model in Table 1. The TC2 predictions are taken from Fig.4 for  $M_{TC} = 300$  GeV and  $K_{UR}^{tc} = 0.4$ , while the predictions of the minimal supersymmetric model are the maximal values taken from [9]. The parameters  $\delta_{LL}$  and  $\delta_{LR}$  parameterize the mixing between top-squarks and charm-squarks and their defini-

tions can be found in [9]. We see that for each channel the TC2 predicts a much larger production rate than the minimal supersymmetric model.

Table 1: The hadronic cross sections of top-quark FCNC productions in TC2 and the minimal supersymmetric model. The TC2 predictions are taken from Fig.4 for  $M_{TC} = 300$  GeV and  $K_{UR}^{tc} = 0.4$ , while the predictions of the minimal supersymmetric model are the maximal values taken from [9]. The corresponding charge-conjugate channels are also included. The LHC sensitivities in the last column are for  $100 \text{ fb}^{-1}$  integrated luminosity.

	SUSY		TC2	LHC sensitivity $3\sigma$
	$\delta_{LL} \neq 0$	$\delta_{LR} \neq 0$		
$gg \rightarrow t\bar{c}$	240 fb	700 fb	30 pb	1500 fb [20, 21]
$cg \rightarrow t$	225 fb	950 fb	1.5 pb	800 fb [18]
$cg \rightarrow tg$	85 fb	520 fb	3 pb	1500 fb [20, 21]
$cg \rightarrow t\gamma$	0.4 fb	1.8 fb	20 fb	5 fb [22]
$cg \rightarrow tZ$	1.5 fb	5.7 fb	100 fb	35 fb [22]

In Table 1 we also list the LHC sensitivity with  $100 \text{ fb}^{-1}$  integrated luminosity. Such sensitivity for each production channel has been intensively investigated in the literature listed in Table 1. Although these sensitivities are based on the effective Lagrangian approach and may be not perfectly applicable to a specified model, we can take them as a rough criteria to estimate the observability of these channels. Comparing these sensitivities with the TC2 predictions, we see that all the productions can be above the  $3\sigma$  sensitivity of the LHC for the chosen TC parameters. But for the minimal supersymmetric model, only the prediction for  $cg \rightarrow t$  is slightly larger than the corresponding LHC sensitivity. Therefore, if these rare processes are observed at the LHC, the TC2 model, rather than supersymmetry, will be favored. Of course, in case of unobservation of these rare productions, the LHC can set meaningful constraints on TC2 parameters.

Note that in Table 1 we did not list the SM predictions, which have not been calculated in the literature

since they must be far below the observable level due to the extremely suppressed top quark FCNC interactions [1]. Also, we did not list the comparison of TC2 and supersymmetry predictions for various top quark FCNC decays, which can be found in the last reference of [7]. From there we see that for top quark FCNC decays the TC2 predictions are also much larger than supersymmetry predictions. So the potentially large top quark FCNC interaction is one characteristic of TC2 model and will serve as a crucial test for this model at future collider experiments.

**Conclusions:** We evaluated the top-quark FCNC productions in the top-color assisted technicolor model at the LHC. These productions proceed respectively by the parton-level processes  $gg \rightarrow t\bar{c}$ ,  $cg \rightarrow t$ ,  $cg \rightarrow tg$ ,  $cg \rightarrow tZ$  and  $cg \rightarrow t\gamma$ . We found that the predictions of the production rates in this model are much larger than in the supersymmetric model and all the productions can be enhanced above the  $3\sigma$  sensitivity of the LHC. Since in the minimal supersymmetric model only  $cg \rightarrow t$  is slightly larger than the corresponding LHC sensitivity, the observation of these processes will imply that the TC2 model is more favored than the supersymmetric model. In case of unobservation of these rare productions, the LHC can set meaningful constraints on TC2 parameters.

**Acknowledgment:** JMY thanks K. Hikasa for helpful discussions and acknowledges the COE program of Japan for supporting a visit in Tohoku University where part of this work is done. This work is supported in part by a fellowship from the Lady Davis Foundation at the Technion, by the Israel Science Foundation (ISF), the National Natural Science Foundation of China under Grant No. 10475107 and 10505007, and by the IISN and the Belgian science policy office (IAP V/27).

- 
- [1] For the FCNC top quark decays in the SM, see, G. Eilam, J. L. Hewett and A. Soni, Phys. Rev. D **44**, 1473 (1991); B. Mele, S. Petrarca and A. Soddu, Phys. Lett. B **435**, 401 (1998); A. Cordero-Cid, *et al.*, Phys. Rev. D **73**, 094005 (2006).
- [2] For a recent review, see, e.g., F. Larios, R. Martinez, M. A. Perez, Int. J. Mod. Phys. A **21**, 3473 (2006).
- [3] M. Paulini, hep-ex/9701019; J. Incandela, FERMILAB-CONF-95/237-E(1995); D. Gerdes, hep-ex/9706001; T. J. Lecompte, FERMILAB-CONF-96/021-E (1996); A. P. Heinson, hep-ex/9605010.
- [4] J. A. Aguilar-Saavedra, Acta Phys. Polon. B **35**, 2695 (2004).
- [5] For FCNC top quark decays in the MSSM, see, C. S. Li, R. J. Oakes and J. M. Yang, Phys. Rev. D **49**, 293 (1994); G. Couture, C. Hamzaoui and H. Konig, Phys. Rev. D **52**, 1713 (1995); J. L. Lopez, D. V. Nanopoulos and R. Rangarajan, Phys. Rev. D **56**, 3100 (1997); G. M. de Divitiis, R. Petronzio and L. Silvestrini, Nucl. Phys. B **504**, 45 (1997); J. M. Yang, B.-L. Young and X. Zhang, Phys. Rev. D **58**, 055001 (1998); C. S. Li, L. L. Yang and L. G. Jin, Phys. Lett. B **599**, 92 (2004); M. Frank and I. Turan, Phys. Rev. D **74**, 073014 (2006); J. M. Yang and C. S. Li, Phys. Rev. D **49**, 3412 (1994); J. Guasch and J. Sola, Nucl. Phys. B **562**, 3 (1999); G. Eilam, *et al.*, Phys. Lett. B **510**, 227 (2001). J.L. Diaz-Cruz, H.-J. He, C.-P. Yuan Phys. Lett. B **179**, 530 (2002); D. Delepine and S. Khalil, Phys. Lett. B **599**, 62 (2004).
- [6] For top-charm associated productions in the MSSM, see, G. Eilam, M. Frank and I. Turan, Phys. Rev. D **74**, 035012 (2006). J. J. Liu, C. S. Li, L. L. Yang and L. G. Jin, Nucl. Phys. B **705**, 3 (2005); J. Guasch, *et al.*, hep-ph/0601218; J. M. Yang, Annals Phys. **316**, 529 (2005); J. Cao, Z. Xiong and J. M. Yang, Nucl. Phys. B

- 651**, 87 (2003).
- [7] For exotic top production processes in TC2 models, see, H. J. He and C. P. Yuan, Phys. Rev. Lett. **83**, 28(1999); G. Burdman, Phys. Rev. Lett. **83**, 2888(1999); J. Cao, Z. Xiong, J. M. Yang, Phys. Rev. D **67**, 071701 (2003); C. Yue, *et al.*, Phys. Lett. B **496**, 93 (2000); J. Cao, *et al.*, Phys. Rev. D **70**, 114035 (2004); F. Larios and F. Penunuri, J. Phys. G **30**, 895(2004); J. Cao, *et al.* Eur. Phys. Jour. C **41**, 381 (2005).
  - [8] For FCNC top quark decays in TC2 theory, see, X. L. Wang *et al.*, Phys. Rev. D **50**, 5781 (1994); C. Yue, *et al.*, Phys. Rev. D **64**, 095004 (2001); G. Lu, F. Yin, X. Wang and L. Wan, Phys. Rev. D **68**, 015002 (2003).
  - [9] J. Cao, *et al.*, Phys. Rev. D **74**, 031701 (2006); hep-ph/0702264.
  - [10] C. Yue, Z. Zong, J. Phys. G **33**, 401(2005); W. Xu, X. Wang, Z. Xiao, hep-ph/0612063.
  - [11] C. T. Hill, Phys. Lett. B **345**, 483 (1995); K. Lane and E. Eichten, Phys. Lett. B **352**, 382 (1995); K. Lane and E. Eichten, Phys. Lett. B **433**, 96 (1998); W. A. Bardeen, C. T. Hill, M. Lindner, Phys. Rev. D **41**, 1647 (1990); G. Cvetic, Rev. Mod. Phys. **71**, 513 (1999).
  - [12] G. Burdman, D. Kominis, Phys. Lett. B **403**, 107 (1997); W. Loniaz, T. Takuch, Phys. Rev. D **62**, 055005 (1999).
  - [13] CDF Collaboration, hep-ph/0612061.
  - [14] R. S. Chivukula, B. Dobrescu, H. Georgi, C. T. Hill, Phys. Rev. D **59**, 075003 (1999).
  - [15] G. 't Hooft and M. J. G. Veltman, Nucl. Phys. B **153**, 365 (1979).
  - [16] T. Hahn, M. Perez-Victoria, Comput. Phys. Commun. **118**, 153 (1999); T. Hahn, Nucl. Phys. Proc. Suppl. **135**, 333 (2004).
  - [17] J. Pumplin, *et al.*, JHEP **0602**, 032 (2006).
  - [18] M. Hosch, K. Whisnant, B. L. Young, Phys. Rev. D **56**, 5725 (1997).
  - [19] C. T. Hill, X. Zhang, Phys. Rev. D **51**, 3563 (1995); C. Yue, Y. P. Kuang, X. Wang, W. Li, Phys. Rev. D **62**, 055005 (2000).
  - [20] T. Han, *et al.*, Phys. Rev. D **58**, 073008 (1998).
  - [21] T. Stelzer, Z. Sullivan, S. Willenbrock, Phys. Rev. D **58**, 094021 (1998).
  - [22] F. del Aguila and J. A. Aguilar-Saavedra, Nucl. Phys. B **576**, 56 (2000).
  - [23] J. A. Aguilar-Saavedra and G. C. Branco, Phys. Lett. B **495**, 347 (2000).